7

Mathematical Modelling of the Motion of Dust-Laden Gases in the Freeboard of CFB Using the Two-Fluid Approach

Alexander Kartushinsky[1] and Andres Siirde[2]
[1]*Tallinn University of Technology, Faculty of Science, Laboratory of Multiphase Media Physics, Tallinn,*
[2]*Tallinn University of Technology, Faculty of Mechanical Engineering, Department of Thermal Engineering, Tallinn, Estonia*

1. Introduction

Fluidized beds are the units designed to provide fluid-solid contacting by the fluid flow through a bed of particles (Andrews and Arthur 2007). A number of thermal processes in technology take advantage of the importance of gas-solid interaction in fluidized beds to carry out gas-solid reactions, heterogeneous catalysis and particle drying. The gas-solid fluidization process in circulating fluidized beds is widely applied in many industrial branches. Characterization of the gas-solid particle flow in a circulating fluidized bed (CFB) riser is important for the process optimization. The particle size distribution has significant influence on the dynamics of gas-solid flow (He et al., 2008) along with another important property of the giving system, such as difference in the physical densities of the used materials. The gas-fluidized beds consist of fine granular materials that are subject to the gas flow from below giving the transport velocity that is large enough to overcome the gravity by the viscous drag force and thus the particles can suspend and be fluidized. When in the fluidized state, the moving particles work effectively as a mixer resulting in a uniform temperature distribution and high mass transfer rate, which are beneficial for the efficiency of many physical and chemical processes (Wang et al., 2005). For this reason the gas-fluidized beds are widely applied in different industries: thermal, energy, chemical, petrochemical, metallurgical, and environmental industries in large-scale operations involving adhesion optimized coating, granulation, drying, and synthesis of fuels and base chemicals (Kunii & Levenspiel, 1991). In general, the lack of understanding of fundamentals of the dense gas–particle flows has led to severe difficulties in design and scale-up of these industrially important gas-solid contactors (van Swaaij, 1985). In most cases, the design and scale-up of fluidized bed reactors is a fully empirical process based on preliminary tests on pilot-scale model reactors, which is a very time consuming and thus expensive activity. Clearly, computer simulations can be a very useful tool to aid this design and scale-up process.

In the CFB furnaces the ash solids and inert materials like sand particles are mainly used as a solid heat carrier – separated in a hot cyclone and cooled after that in a heat exchanger

while the ash particles come back into the furnace. The temperature level in the furnace can be held in the given range by circulating the ash/sand masses. While the heat capacity of ash is quite low, the circulating ash mass must be huge. One way of optimization is to keep up higher heat capacity by adding inertial sand particles. The high ash concentration in furnace gases can be attained with i) high velocity of gas in bed when the fuel particles carried out of bed are burned and their ash fills the whole volume of furnace and ii) ash circulation. The CFB combustion technology enables to bind the sulphur components with the carbonate components added to the fuel or existing within the mineral part of the fuel. A disadvantage of CFB is that some fuel ash particles become too fine during the circulation and therefore the size of ash particles contained in the fuel gas exiting the hot cyclone is too small. As a result of disintegration, the mass of fine ash particles, which are not separated from flue gases or captured in the connective flue ducts and multicyclone increases. The high concentration of particles in the fire gases of CFB furnace chamber contributes to the formation of particle clusters with the solid phase concentration within 0.1 – 0.2 m^3/m^3. At the exit of CFB boiler furnace the density of solid phase is within 5 – 20 kg/m^3.

The given paper is an advanced research of two previous references: "Numerical simulation of uprising gas-solid particle flow in circulating fluidized bed" (Kartushinsky et al., 2009) and "Numerical simulation of uprising turbulent flow by 2D RANS for fluidized bed conditions" (Krupenski et al., 2010) where the mathematical modelling of CFB has been performed. The first one is related to the numerical simulations of CFB where the two-phase turbulent boundary layer approach (TBL) was included. The latter concerns modelling of CFB processes by the RANS approach, which has been developed for both, the gaseous and solid phases, implementing the Euler/Euler approximations or a two-fluid model. Both papers have their advantages and disadvantages. For instance, in the TBL approach the diffusive source terms were retained only in one direction, namely, in the transverse direction, and the magnitude of average transverse velocity components in the gas- and dispersed phases were much less than that of longitudinal components of the corresponding velocities in the gas- and dispersed phases. Such an approach is fully valid and used in the pipe channel flows as well as in the turbulent round jets and flows past the rigid shapes (Hussainov et al., 1995, 1996, Frishman et al., 1997). Nevertheless, a more rigorous and accurate solution was obtained with the help of RANS approach where there are no artificial predictions attached to the TBL approach. However, in both papers only one component of solid admixture, namely, the ash particles are used to simulate the motion of particulate solid phase as a whole.

The current mathematical performance assesses the effect of the presence of two coexisting solid substances, such as ash (light) and sand (heavy) particles with the particle size distribution for each component of solids. This system represents one step further for the mathematical approach to capture real physical processes in CFB. Besides, by making calculations in the real CFB conditions (high temperature of the process) we take into account the amount of heat that must be separated from the combustor by the sensible heat of ash and solid sand particles. The approach enables to optimize particle mass concentration of ash and sand solid particles in fire gases.

The problem is solved by using elaborated mathematical modelling with the help of 2D RANS approach that applies to two coexisting phases. The numerical simulations are performed in the vertical freeboard CFB flow conditions when the temperature of carrier gas-phase fluid is 1123K. Therefore the corresponding magnitudes of parameters of the gaseous phase such as kinematic viscosity coefficient and density of the gaseous phase must

be increased by the factor ten and decrease by factor three, respectively, versus their magnitudes obtained for the normal flow conditions at the temperature 293K.
The following practical initial data were used in calculations:

Generic name		*Dimension*	*Minimal*	*Average*	*Maximal*
Pipe data	**Diameter**	m	0.0305	0.0305	0.0305
	Height	m	1.525	1.525	1.525
Ash concentration		kg/nm^3	10	20	20
Ash density		kg/m^3	2000	2000	2000
Ash particle size		m	0.005	0.0075	0.01
Sand density		kg/m^3	2600	2600	2600
Sand particle size		m	0.005	0.0075	0.01

Table 1. The initial data for calculations.

For these media we have chosen the initial data very close to the medium in the Estonian oil-shale CFB furnace. The problems of two-phase flows in the CFB risers have been analyzed in certain publications (Hussain et al., 2005, Moscow Energija, 1973), but these studies do not consider dependence of the amount of sensible heat carried by solid particles on the mass flow loading magnitude. The numerical parametric study deals with the influence of the parameters of various riser exits on the hydrodynamics of gas-solid two-phase flow in the CFB riser (Hussain et al., 2005, Moscow Energija, 1973).
The freeboard CFB used in the given research represents a cylindrical symmetric pipe flow domain occupied by the giving mixture of gas and two types of solid particles. Since the two-fluid model or Euler/Euler approach is applied for the description of the behaviour of solid particles as continuous co-existing phases, the numerical performance is carried out with the finite (control) volume method (Perić & Scheuerer, 1989 and Fertziger & Perić, 1996) written in numerical codes. Another mathematical modelling method, which also operates with the Euler/Euler (or coexisting) approximation deals with the high density or packed particulate flows and solution is obtained with applying the theory of granular flows, for example, that by book of Multiphase Flow and Fluidization: *Continuum and Kinetic Theory Descriptions* (Gidaspov, 1994). In such particulate flows, the particle-turbulence interaction phenomenon is less significant in comparison with the particle-particle collision phenomenon. On the contrary to the Euler/Euler approach, another well-known approximation, which is frequently applied for modelling, the dispersed phase is the Lagrangian Particle Tracking method. The Lagrangian method deals usually with huge numbers of tracking particles (up to several millions of tracking particles depending on the mass flow loading) to obtain a converged solution and also to take into account the particles feedback in the primary fluid (gas-phase). One mathematical technique that can be used for the calculation of flow parameters, including the coupling effect, is given by the particle-cell source method (Crowe et al., 1977). Helland et al., (2000) using the Lagrangian Particle-Tracking approach to calculate the two-dimensional gas-solid particles flow in a CFB riser with the 3% total volume concentration of solids. To take into account the effect of the inter-particle collisions within the Lagrangian approach, (Sommerfeld, 2001) developed a stochastic inter-particle collision model with the introduction of a fictitious particle with which the traced particles might collide.

To sum up with introduction one can underline an importance of sought problem, that is the key study of given process is taken place in freeboard of furnace of CFB steam-generator and which is under numerical investigation.

2. Theoretical terms of the model

2.1 Governing equations for the two dimensional RANS model

In the area of multiphase flows there has been developed a lot of models for particulate flows in several papers e.g.(Pfeffer et al., 1966, Michaelides, 1984). A "two-fluid model" is being used in the modelling of dispersed two-phase systems where the gas and particles are considered as two coexisting phases that reach the entire flow domain. To describe the flow of the particulate phase, one of the possibilities is using the Reynolds-Averaged Navier-Stokes (RANS) method. The general equations of this method were examined by plenty of experiments, which showed that with using this method it is possible to discover, for example, the boundary conditions using the wall-functions approach and it is quite easy to implement it numerically. In this work the RANS method is used for both coexisting phases, namely the gas- and solid phases with the closure equations. Two basic predictions were used for closure of the governing equations of gaseous and dispersed phases:
i) the four-way coupling model (Crowe, 2000) by that captures one capture the particle-turbulence interaction phenomena and ii) the inter-particle collision closure model (Kartushinsky & Michaelides 2004) to assess an the particles interaction. The both models are used for receiving an output of necessary data which are the axial and radial velocities, turbulent energy and the particle mass concentration. The information on these parameters will be much useful for evaluation of the relevant processes occurred in particulate flows like CFB processes.
This model is based on the complete averaged Navier-Stokes equations applied for the axisymmetrical upward gas-solid particle turbulent flow in the freeboard CFB processes. The governing equations present the carrier fluid (gas-phase) and solid (polydispersed) phase which is considered a co-existing flow and consists of a continuity equation for the gas-phase and mass conservation equation in the dispersed phase together with the momentum equations for both phases in the longitudinal and radial directions. In addition, the moment of momentum equation is included for the solid phase because of Magnus lift force and plausible particle rotation stemmed from the wall interaction. The solid phase is considered a polydispersed phase, which consists of two particle fractions – light (ash) particles and heavy (sand) particles. The present governing equations along with the corresponding boundary conditions are given by Kartushinsky and Michaelides (2004, 2006, 2009) and are the following:

1. Continuity for the gaseous phase:

$$\frac{\partial u}{\partial x}+\frac{\partial (rv)}{r\partial r}=0 \tag{1}$$

2. Linear momentum equation in the longitudinal direction for the gaseous phase:

$$\frac{\partial}{\partial x}\left(u^2-\nu_t\frac{\partial u}{\partial x}\right)+\frac{\partial}{r\partial r}r\left(uv-\nu_t\frac{\partial u}{\partial r}\right)=-\frac{\partial p}{\rho\partial x}+\frac{\partial}{\partial x}\nu_t\frac{\partial u}{\partial x}+\frac{\partial}{r\partial r}r\nu_t\frac{\partial v}{\partial x}$$

$$-\sum_{i=1,3}\alpha_i\left(\frac{u_{ri}}{\tau'_i}+C_{Mi}\Omega_i v_{ri}\right) \tag{2}$$

3. Linear momentum equation in the radial direction for the gaseous phase:

$$\frac{\partial}{\partial x}\left(uv-\nu_t\frac{\partial v}{\partial x}\right)+\frac{\partial}{r\partial r}r\left(v^2-\nu_t\frac{\partial v}{\partial r}\right)=-\frac{\partial p}{\rho\partial r}+\frac{\partial}{\partial x}\nu_t\frac{\partial u}{\partial r}+\frac{\partial}{r\partial r}r\nu_t\frac{\partial v}{\partial r}$$

$$-\frac{2\nu_t v}{r^2}-\sum_{i=1,3}\alpha_i\left(\frac{v_{ri}}{\tau'_i}-(C_{Mi}\Omega_i+F_{si})u_{ri}\right) \tag{3}$$

4. Turbulence kinetic energy equation for the gaseous phase:

$$\frac{\partial}{\partial x}\left(uk-\nu_t\frac{\partial k}{\partial x}\right)+\frac{\partial}{r\partial r}\left(vk-\nu_t\frac{\partial k}{\partial r}\right)=$$

$$\nu_t\left\{2\left[\left(\frac{\partial u}{\partial x}\right)^2+\left(\frac{\partial v}{\partial r}\right)^2+\left(\frac{v}{r}\right)^2\right]+\left(\frac{\partial u}{\partial r}+\frac{\partial v}{\partial x}\right)^2\right\}$$

$$-\varepsilon_h+\sum_{i=1,3}\frac{\alpha_i}{\tau_i}\left(u_{ri}^2+v_{ri}^2+0.5(\overline{u'^2_{si}}+\overline{v'^2_{si}})\right) \tag{4}$$

5. Mass conservation equation for the solid phase:

$$\frac{\partial}{\partial x}(\alpha_i u_{si})+\frac{\partial}{r\partial r}(r\alpha_i v_{si})=-\frac{\partial}{\partial x}\left(D_{si}\frac{\partial\alpha_i}{\partial x}\right)-\frac{\partial}{r\partial r}\left(rD_{si}\frac{\partial\alpha_i}{\partial r}\right) \tag{5}$$

6. Momentum equation in the longitudinal direction for the solid phase:

$$\frac{\partial}{\partial x}(\alpha_i u_{si}u_{si})+\frac{\partial}{r\partial r}(r\alpha_i u_{si}v_{si})=$$

$$-\frac{\partial}{\partial x}\left(\alpha_i\overline{u'^2_{si}}\right)-\frac{\partial}{r\partial r}\left(r\alpha_i\overline{u'_{si}v'_{si}}\right)+\alpha_i\left[\frac{u_{ri}}{\tau'_i}+C_{Mi}\Omega_i v_{ri}-g\left(1-\frac{\rho}{\rho_\rho}\right)\right] \tag{6}$$

7. Momentum equation in the radial/transverse direction for the solid phases:

$$\frac{\partial}{\partial x}(\alpha_i v_{si}u_{si})+\frac{\partial}{r\partial r}\left(r\alpha_i v^2{}_{si}\right)=$$

$$-\frac{\partial}{\partial x}\left(\alpha_i\overline{u'_{si}v'_{si}}\right)-\frac{\partial}{r\partial r}\left(r\alpha_i\overline{v'^2_{si}}\right)+\alpha_i\left[\frac{v_{ri}}{\tau'_i}-(C_{Mi}\Omega_i+F_{si})u_{ri}\right] \tag{7}$$

8. Angular momentum equation for the solid phases:

$$\frac{\partial}{\partial x}\left(\alpha_i \omega_{si} u_{si}\right) + \frac{\partial}{r\partial r}\left(r\alpha_i \omega_{si} v_{si}\right) =$$

$$-\frac{\partial}{\partial x}\left(\alpha_i \overline{u'_{si}\omega'_{si}}\right) - \frac{\partial}{r\partial r}\left(r\alpha_i \overline{v'_{si}\omega'_{si}}\right) - \alpha_i C_{\omega i}\frac{\Omega_i}{\tau_i} \tag{8}$$

Here p is the pressure, u, u_s, v_s, ω_s are the longitudinal, radial, angular velocity components of gas- and solid phases (subscript s), respectively, and α the particle mass concentration. The subscript "i" corresponds to the number of particle fraction and varies in the range ($1 \le i \le 3$), which composes the polydispersed phase. The particle void fraction is linked with the particle mass concentration as $\alpha = \beta\rho / \rho_p$ (β is solids void fraction). The closure equations of gas-phase are performed by using $k - L_h$ four-way coupling model of Crowe (2000) where k is the turbulent energy of carrier fluid and L_h is the hybrid length scale. This parameter is computed as a harmonic average of the integral turbulence length scale of single phase pipe flow, L_0 ($L_0 = k_0^{3/2} / \varepsilon_0$) and inter-particle spacing, λ, defined as $\lambda = \delta\sqrt[3]{\left(\rho_p / \alpha\rho\right) - 1}$. Thus, the hybrid length scale or scale of dissipation rate of turbulent energy in particulate flows is determined as $L_h = 2L_0\lambda / \left(L_0 + \lambda\right)$ [Crowe 2000]. The values, ρ_p and ρ are the densities of the particle materials and gas-phase, δ is the particle size. The coefficient of turbulent viscosity is calculated as $\nu = \sqrt{k}L_0$, by the turbulent energy of particulate flow and turbulence length scale related to the single phase flow. Thus, the parameters of the single phase flow (subscript 0), the average velocity components, turbulent energy, k_0, its dissipation rate, ε_0, together with L_0 (while $T_0 = k_0 / \varepsilon_0$ is integral turbulence time scale) have to be calculated in advance (in preliminary calculations) for completion modelling in the pipe gas-solid turbulent flow system. An advantage of the four-way coupling model of (Crowe, 2000) (with the inclusion of particle collision) is that it includes the turbulence enhancement by the presence of particles, expressed via the term $\frac{\left(u_r^2 + v_r^2\right)}{\tau}$ ($u_r = u - u_s$ and $v_r = v - v_s$ is the slip velocity between the gas- and solid phases along the streamwise and radial directions) and turbulence attenuation via the increase of its dissipation rate by particles, $\varepsilon_h = k^{3/2} / L_h$ (in the right-hand side terms of Eq. 4). $\tau = \frac{\rho_p \delta^2}{18\rho\nu}$ is the particle response time for the Stokes regime (ν is the kinematic viscosity coefficient) and $\tau' = \tau / C'_D$ for the non-Stokes regime expressed via the particle Reynolds number, $\mathrm{Re}_s = \delta\sqrt{u_r^2 + v_r^2} / \nu$ and $C'_D = 1 + 0.15\mathrm{Re}_s^{0.687}$. By determining of the coefficients of C_{Mi} and F_{si} one can correct the values of the lift Magnus and Saffman forces and $C_{\omega i}$ for the particles rotation are taken from (Crowe et al., 1998) for relevant range of change of the particle Reynolds number, Re_s. $\Omega = rot\vec{V} - \omega_s$ is the angular velocity slip of particles while

the differential mathematical operator "rot" over the gas velocity vector $\vec{V}$ is defined for the 2D motion, as $rot\vec{V} = \frac{1}{2}\left(\frac{\partial v}{\partial x} - \frac{\partial u}{\partial r}\right)$. The average values, $\overline{\alpha' u_s'}$, $\overline{\alpha' v_s'}$, $\overline{u_s'^2}$, $\overline{v_{si}'^2}$, $\overline{u_s' v_s'}$, $\overline{u_s' \omega_s'}$, and $\overline{v_s' \omega_s'}$ are the particles stress tensors originated from their turbulent fluctuation along with their inter-collisions calculated from (Kartushinsky & Michaelides, 2004). Due to the particle turbulent diffusion and particle collision the diffusion coefficient has two components: $D_s = D_{sturb} + D_{col}$. The first term in expression for the particle diffusion coefficient is calculated as $\mathrm{D_{sturb}} = \frac{2}{3}\mathrm{k}\left(\tau + \mathrm{T_0}\right)\left[1 - \exp\left(-\frac{\mathrm{T_0}}{\tau}\right)\right]$ from the PDF model of Zaichik & Alipchenkov (2005) and the second term is taken from the particle's collision model of Kartushinsky & Michaelides (2004).

3. Results and discussions

The numerical method: In the given RANS computations the *control volume* (cv) method was used. The governing equations (1-9) were solved using a strong implicit procedure with the lower and upper matrix decomposition and up-wind scheme for convective fluxes (Perić & Scheuerer, 1989 and Fertziger & Perić, 1996). For the considered computations, 145,000 uniformly distributed control volumes were utilized for running the numerical codes. The wall functions were incorporated at a dimensionless distance from the wall as follows, $\mathrm{y^+} = \frac{\Delta y \cdot v_*}{\nu} = \frac{\Delta y \cdot c_\mu \sqrt{k}}{\nu} = 10$, where Δy and c_μ are the control volume size and the empirical constant that equals to $c_\mu = 0.09$ and k is the turbulent energy, respectively.

All computations were extended from the pipe entrance to a short distance up to *x/D=50* (D is the pipe diameter) similar to the height of the freeboard of CFB. For the particulate phase, when the size of particles is often larger than the size of the viscous boundary sub-layer, the volume domain occupied by the dispersed phase has slightly shrunk, which gives always positive values for the solids' velocities in the wall vicinity. This method follows the numerical approach by Hussainov et al., (1996) has been employed here.

All results are presented in the dimensionless way: the velocities of both phases are related to the gas-phase velocity at the centre of the flow (r=0), the turbulent energy is normalized to a square of the gas-phase velocity, and particle mass concentration is normalized to its value at (r=0).

The numerical results. The effect of inter-particle collisions is very important for the particulate flows when the ratio of $\tau_c / \tau < 1$ (where τ_c is the time of inter-particle collision and τ is the particle response time). In the considered freeboard CFB, for the particulate flows with a high mass flow ratio about or above 10kg dust/kg air the given ratio of τ_c / τ is less unit resulted in accounting of the collision process in CFB by utilizing "collision terms" in equations (5-8). These terms are responsible for inter-particle collisions. These are terms for the production of longitudinal and radial components of linear velocity correlations and deriving linear and angular velocity correlations of the solid phase, such as $\overline{u_s'^2}$, $\overline{v_{si}'^2}$, $\overline{u_s' v_s'}$, $\overline{u_s' \omega_s'}$, $\overline{v_s' \omega_s'}$. These velocity correlations are due to the particle collision between various fractions and they are computed from the difference in average velocities

of various sizes of particles and from that in particle material densities (light and heavy particles). An analytical expression for given velocity correlations of the dispersed phase along with the closure approach of the governing equations of polydispersed phase, Eqs. (5-8), are given in model of (Kartushinsky & Michaelides, 2004).

The results of numerical simulation are shown in the following Figures 1-7. The axial velocity distribution of dispersed phase is calculated as an average velocity of the mixture of ash particles of different sizes or as a mixture of ash and sand particles with applying the formulae, $\overline{u_s} = \sum_i \alpha_i u_{si} / \sum_i \alpha_i$ where u_{si}, and α_i are the axial linear velocity and particle mass concentration of ash or ash and sand particles, respectively. The Fig.1 shows longitudinal distribution of the gas- and solid phases for three examined cases: mixture1 is the ash ($\rho_p = 2000 \text{kg/m}^3$) and sand particles ($\rho_p = 2600 \text{kg/m}^3$) of the same size, 500μm with the total mass flow loading of 10kg/kg equally distributed between the ash and sand particle fractions; mixture2 is the composition of ash particles of two sizes, 500 and 1000μm and sand particles of 500μm with the total mass flow loading of 10kg/kg, which are equally distributed between these three particle fractions, and finally, mixture3 consists of ash and sand particles of the same size 500μm with the higher total mass flow ratio of 20kg/kg where the mass fractions are equally distributed between the ash and sand particles. The calculations were performed for the conditions of CFB, namely, when the density of the gaseous carrier fluid was ρ=0.3kg/m^3 and kinematic viscosity of the carrier fluid $\nu = 1.5 \cdot 10^{-4}$ m^2/s. This corresponds to the flow parameters of hot gases at the temperature of T=1123K.

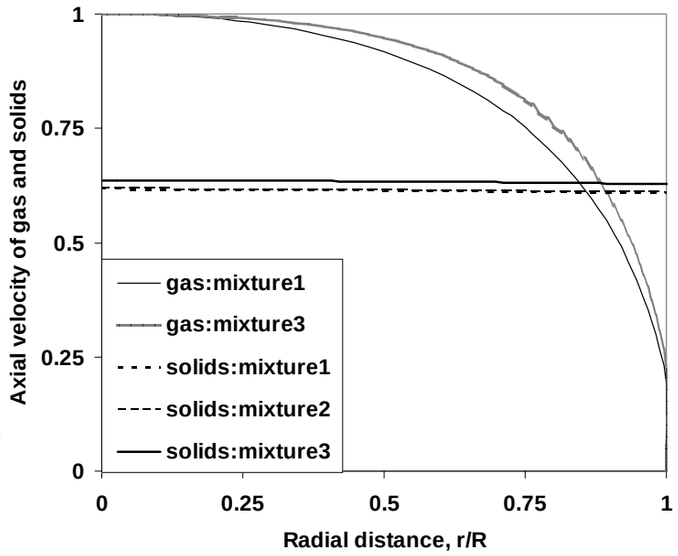

Fig. 1. Axial velocity distribution of gas- and dispersed phases for their average axial velocity by different flow conditions for mixtures 1, 2 and 3.

As one can notice, the gas velocity profile is similar to the typical turbulent velocity profile, however in a dense flow with high mass loading, e.g., 20kg/kg loaded by coarse particles, the velocity profile of the carrier gas-phase becomes flatter (diffusive line in Fig.1). It comes from the effect of turbulence enhancement by the motions of coarse particles, which modify

the velocity profile to its shape of "fully" turbulent regime. At the same time the average magnitude of the longitudinal velocity component of solids slightly increases with the growth of the mass flow ratio (cf. straight dashed and bold solid lines in Fig. 1). Such tendency in the two-phase turbulent jet has been experimentally observed by Laats & Mulgi (1979). Fig. 1 gives also the distribution of longitudinal velocity components of different solid particles. As the modelling shows, the velocity distribution of solid phase is less sensible to the variation of particle sizes than to the change of mass flow loading (cf. longitudinal velocity profiles for mixture1 and mixture3, straight lines in Fig. 1).
The following Figs. 2 and 3 show the detailed distribution of longitudinal velocity components for each particle fraction of solids presented separately. The cases of mixture1 and mixture3 show similar particle sizes of 500μm, but different material densities (light and heavy particles) and also different mass flow ratios: 10 and 20kg/kg (Fig. 2). The other cases are the mixture1 and the mixture2 with the particle sizes and material densities distributions obtaining for the same total mass flow loading 10kg/kg (Fig. 3). As one can notice, the ash particles have higher velocity than heavy sand particles (cf. dashed and solid dashed lines, Fig.2) that could be observed for both mass flow loadings: 10kg/kg (mixture1) and 20kg/kg (mixture3). Mixture2 is a more complicated case of particle composition. Considering the above, we can see that the larger ash particles have a lower velocity value than the smaller ones (cf. light and dark diffused lines for 500 and 1000μm particles, Fig.3). However, at the same time the heavier sand particles of 500μm have larger velocity magnitude than the lighter ash particles of 500 and 1000μm, which show smaller velocity magnitude (Fig.3). This trend is probably caused by the higher rate of particle collision between the light ash particles of different sizes than that between the light and heavy particles of the same size. It is difficult to predict such a tendency, but, it can be observed in numerical simulations.

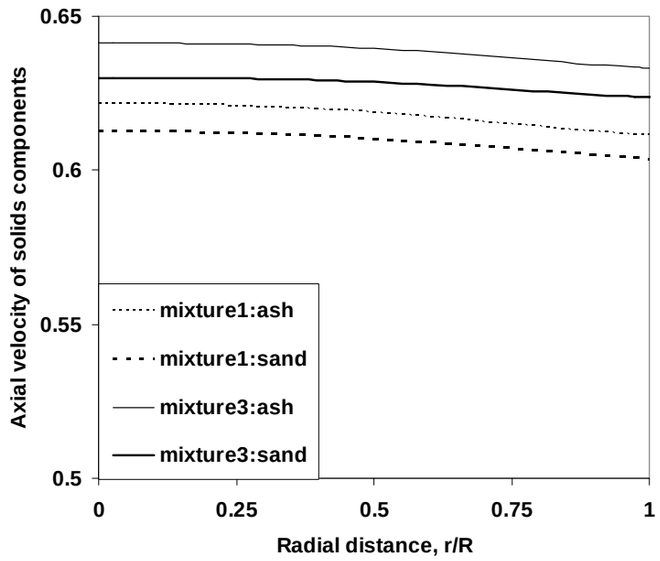

Fig. 2. Axial velocity profiles of ash and sand particles for various flow conditions: mixture1: ash and sand particles of 0.5mm for 10kg/kg and mixture3: ash and sand 0.5mm for 20kg/kg.

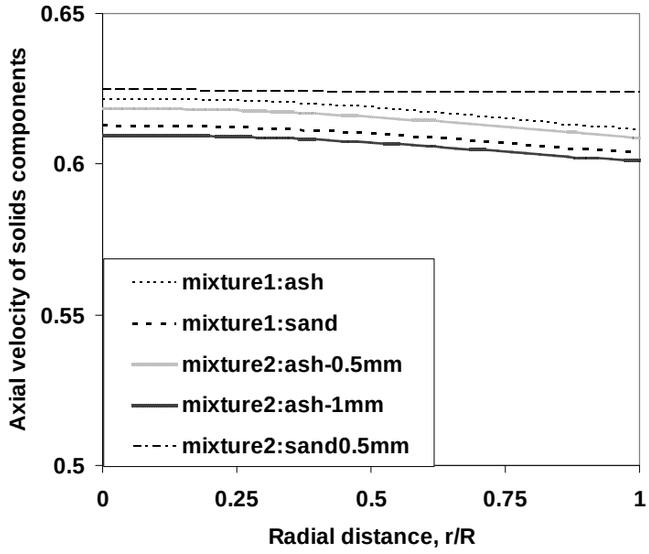

Fig. 3. Axial velocity profiles of ash and sand particles for various flow conditions: mixture1: ash and sand particles of 0.5mm and mixture2: ash 0.5 and 1mm and sand 0.5mm for 10kg/kg.

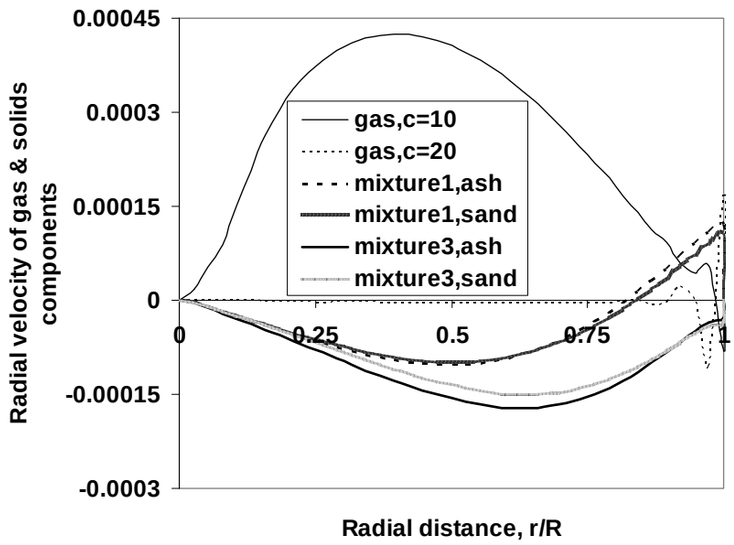

Fig. 4. Radial velocity profiles of gas phase and two components of solids for various flow conditions: mixture1 and mixture3 for ash and sand solid phases with different mass loadings, 10 and 20 kg/kg, respectively.

Fig. 4 shows the distribution of radial velocity components of gas- and dispersed phases. The profiles of radial velocities of ash and sand particles have been plotted separately for different mass loadings: 10 (mixture1) and 20kg/kg (mixture3). As one can notice, increase of mass flow loading results in change of shape and magnitude of the radial gas velocity

profile (cf. dashed and solid lines, Fig. 4). Different behaviour in the distribution of radial velocity components of solid and gas-phase can also be observed. Namely, the profiles of solid phase have concave shape while the profile of gas-phase is convex. This means that the increase of mass flow loading results in the increase of radial velocity component of both fractions whatever particles are considered – the ash or sand particles (cf. solid and diffused lines for mixture3 versus the dashed bold and diffused bold lines for mixture1, Fig. 4). This comes from the effect of attenuation of the gas-phase by a larger amount of solid particles in the flow.

The effect of lift forces is given in Fig. 5 in terms of the distribution of angular velocity of particles. Fig. 5 shows the distribution of angular velocity of ash and sand particles separately and also their average angular velocity calculated analogously to the above-mentioned calculation of average linear velocity of solids in the given form: $\overline{\omega_s} = \sum_i \alpha_i \omega_{si} / \sum_i \alpha_i$ where ω_{si} is the angular velocity of composed particle fractions. As the figure shows, the angular velocity of particles is gradually increasing towards the wall and light ash particles have higher rotation in the vicinity of the wall than heavy sand particles. The increase of particle rotation is obviously stemmed from effect of diminishing of the particles inertia. The particle rotation results indirectly from the intensification of the mixing process, because of the growth of Magnus lift force that causes the particle migration across the flow.

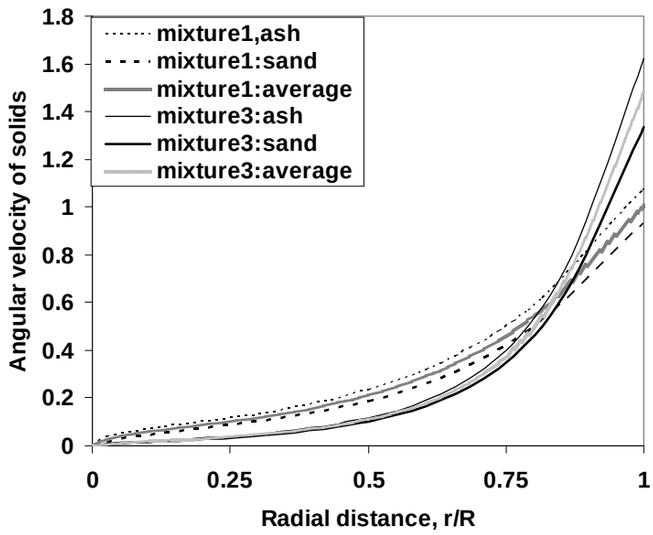

Fig. 5. Angular velocity profiles of ash and sand particles and average profile of the mixture of particles $\overline{\omega_s}$ for the same flow conditions in Fig. 4 for mixtures 1 and 3.

Fig. 6 shows the distribution of particle mass concentration across the two regimes of the flow, which depends on the mass flow ratio: mixture1 with 10kg/kg and mixture3 with 20kg/kg. As the figure shows the lower mass flow ratio results in the slower decrease of mass concentration towards the wall versus the increase of mass concentration of particles for higher mass loading of the flow. As numerical results show, the profile of particle mass concentration is close to the flat shape, which can be observed in the flow loaded by coarse

particles. In fact, the numerically obtained profiles of particle mass concentration are highly appreciated because of the efficient operation of CFB units. On the contrary, in the flow domain the gradient profiles of mass concentration can cause retard of enhancement of the combustion process. Thus, an additional sand mass fraction brought to the flow domain may contribute to the improvement of the combustion process in CFB cycles.

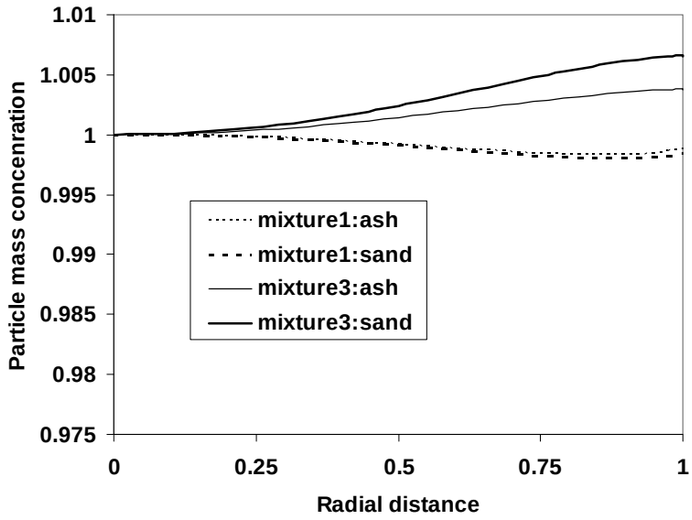

Fig. 6. Distribution of particle mass concentration for ash and sand solid phases in different flow conditions shown in previous Figs. 4 and 5: for mixtures 1 and 3.

Finally, the Fig. 7 shows distribution of turbulent the energy across the flow. All considered results for given three different regimes: mixture1, mixture2 and mixture3 are matched between each other and versus also turbulent energy of single phase flow. As a whole, the trend shows that the particles in all the observed regimes generate the turbulence, which stems from the vortex shedding phenomenon behind the particles which is input to the level of turbulence generated by the flow itself. This effect of turbulence modulation, namely, the turbulence enhancement due to the presence of coarse particles is explained and computed using the four-way coupling model by Crowe (2000). This amount of an additional turbulent energy is proportional to the square of velocity slip between the gaseous and the solid phases following the model by Crowe (2000) and it is substantial because of large velocity slip between the phases owing to high inertia of large particle size. Following to the model of Crowe (2000), this generation term is balanced by the introduced dissipation rate of turbulent energy and calculated via the hybrid turbulence length scale (last term in the right-hand side of Eq. 5). The given four-way coupling model by Crowe (2000) is based on the criteria of turbulence modulation by particles considering the ratio of particle size to the integral turbulence length scale. In accordance with this criterion for the considered cases of two-phase turbulent flow loaded by 500 and 1000μm particles, this scale ratio is far above 0.1 and therefore the particles enhanced the turbulence of the carrier gas-phase flow. In addition, the effect of increase of polydispersity grade, i.e. particle size variation from 500 up to 1000μm occurred for the mixture2 (only with ash particles) is less pronounced than that with increase of mass flow ratio up to 20kg/kg occurred in the case of the mixture3 (cf. bold dashed line in Fig. 7), on forming the shape and magnitude level of turbulent energy.

Feeding of particles into the flow field may create some reason for additional turbulence generation and it is much appreciated because the intensification of mixing process in CFB can be substantially improved, and as a result, higher efficiency of the combustion process in CFB units can be obtained.

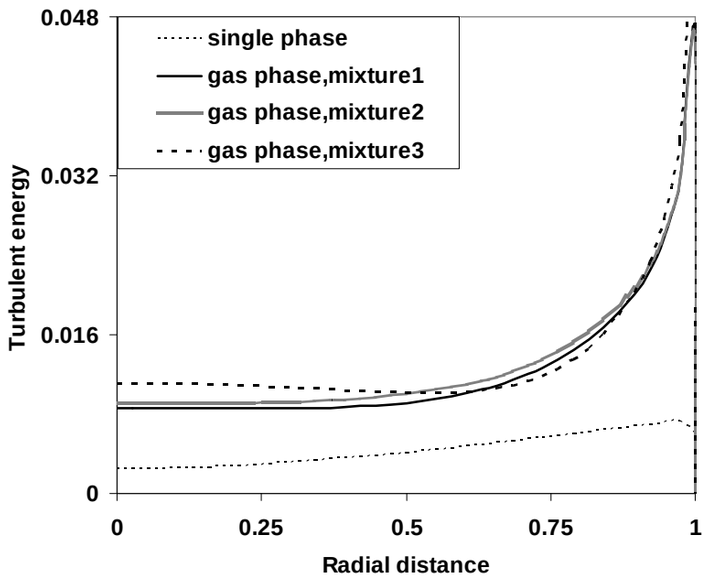

Fig. 7. Turbulent energy profiles of single and gas phases for mixtures 1, 2 and 3 with different particle sizes of ash: 0.5 and 1 mm and sand 0.5 mm and for the mass loadings (10 and 20 kg/kg).

4. Comparison of the results

Comparing the results with our previous research (Kartushinsky et al., 2009 and Krupenski et al., 2010) in which the theoretical initial data were used we can notice the following perceptible fact:
Inclusion of second (heavier) particle fraction modifies the turbulence of carrier fluid resulting in the intensification of mixing process in the freeboard area of CFB.

5. Conclusions

The numerical study of particulate turbulent flow modelled by 2D RANS (Euler/Euler) approach showed importance of addition of second solid fraction, characterized by heavy (sand) particles along with existence of first solid fraction of lighter (ash) particles in the mixing process taken place in freeboard CFB process. The main contribution to the flow formation stems from the inclusion of inter-particle collisions and four-way coupling turbulence modulation due to the presence of polydispersed solid particles with various physical properties. Other forces exerted on the motion of solids are: the gravitation, viscous drag and lift forces. On the basis of the performed calculations one can conclude:

a. variation of solids material properties results in the enhancement of flow turbulence in comparison with the turbulence level of the flow loaded by one particle fraction;

b. increase of mass loading of the flow is more pronounced for turbulence enhancement than the increase of particle size;
c. increase of mass flow ratio intensifies the mixing process resulting in uniform distribution of mass concentration of solids;

The obtained results can be implemented for updating/refurbishing of the industrial scale CFB risers using the real sizes distribution of solid particles of ash and sand for the combustion of Estonian oil-shale particles.

6. Acknowledgements

The work was support from target financing of the Project SF0140070s08 (Estonia). The authors are grateful for the technical support of cluster computers from the Universities of Texas at Austin and San Antonio (USA).

7. References

Andrews, A.T. (2007). IV Filtered Models for Gas-Particle Flow Hydrodynamics. *PhD Thesis,* 235 pages.

Crowe, C.T.; Stock, D.E. & Sharma, M.P. (1977). The Particle-Source-In Cell "PSI-CELL" Model for Gas-Droplet Flows. *ASME Transactions*, *Series I - Journal of Fluids Engineering*, Vol.99, 325-332.

Crowe, C.; Sommerfeld, M. & Tsuji, M. (1998). *Multiphase Flows with Droplets and Particles*. CRC Press LLC, Boca Raton, Florida. ISBN 0-8493-9469-4.

Crowe, C.T. (2000). On Models for Turbulence Modulation in Fluid-Particle Flows. *International Journal of Multiphase Flow*, Vol.26, No.5, pp. 719-727.

He, Y.; Deen, N.G.; van Sint Annaland, M. & Kuipers, J.A.M. (2008). Gas-Solid Turbulent Flow in a Circulating Fluidized Bed Riser; Numerical Study of Binary Particles Mixtures, *9th International Conference on Circulating Fluidized Beds*, Germany.

Fertziger, J.H. & Perić, M. (1996). *Computational Method for Fluid Dynamics*. Springer-Verlag Berlin Heidelberg. ISBN 3540594345.

Frishman, F.; Hussainov, M.; Kartushinsky A. & Mulgi A. (1997). Numerical Simulation of a Two-Phase Turbulent Pipe-Jet Flow Loaded with Polyfractional Solid Admixture. *International Journal of Multiphase Flow*, Vol.23, No.4, pp. 765-796.

Gidaspov, D. (1994). *Multiphase Flow and Fluidization: Continuum and Kinetic Theory Description*. Boston: Academic Press. ISBN 10: 0-12-282470-9.

Helland, E.; Occelli, R. & Tradist, L. (2000). Numerical study of cluster formation in a gas-particle circulating fluidized bed. Power Technology, Vol.110, No.3, pp. 210-221.

Hussainov, M.; Kartushinsky, A.; Mulgi, A.; Rudi Ü. & Tisler, S. (1995). Experimental and Theoretical Study of the Distribution of Mass Concentration of Solid Particles in the Two-Phase Laminar Boundary Layer on a Flat Plate. *International Journal of Multiphase Flow*, Vol.21, No.6, pp. 1141-1161. ISSN 0301-9322.

Hussain, A.; Ani, F. N.; Darus, A. N.; Mustafa, A. & Salema, A. A. (2005). *Proceedings of the 18th International Conference on Fluidized Bed Combustion*, ASME Publication, pp. 1-7.

Hussainov, M.; Kartushinsky, A.; Mulgi, A. & Rudi, Ü. (1996). Gas-solid flow with the slip velocity of particles in a horizontal channel. *Journal of Aerosol Science*. Vol.27, No.1, pp. 41-59.

Kartushinsky, A. & Michaelides, E.E. (2004). An Analytical Approach for the Closure Equations of Gas-Solid Flows with Inter-Particle Collisions. *International Journal of Multiphase Flow*, Vol.30, No.2, pp. 159-180.

Kartushinsky A. & Michaelides, E.E. (2006). Particle-laden gas flow in horizontal channels with collision effects. *Powder Technology*, Vol.168, pp. 89-103.

Kartushinsky, A.; Michaelides, E.E. & Zaichik, L.I. (2009). Comparison of the RANS and PDF Methods for Air-Particle Flows. *International Journal of Multiphase Flow*, Vol.35, pp. 914-923.

Kartushinsky, A.; Martins, A.; Rudi, Ü.; Shcheglov, I.; Tisler, S.; Krupenski, I. & Siirde, A. (2009). Numerical Simulation of Uprising Gas-Solid Particle Flow in Circulating Fluidized Bed. *Oil-Shale*, Vol.26, No.2, pp. 125-138.

Krupenski, I.; Kartushinsky, A.; Siirde, A. & Rudi, Ü. (2010). Numerical Simulation of Uprising Turbulent Flow by 2D RANS for Fluidized Bed Conditions. *Oil-Shale*, Vol.27, No.2, pp. 147-163.

Kunii, D. & Levenspiel, O. (1991). *Fluidization Engineering*. Butterworth Heinemann E.U.A. (Ed), London, UK.

Laats, M.K. & Mulgi, A.S. (1979). Experimental Investigation of Kinematic Picture of Solid Particles in Pipe Flow. *Proceedings of Estonian Academy of Sciences*, Tallinn, pp. 32-46 (in Russian).

Michaelides, E.E. (1984). A Model for the Flow of Solid Particles in Gases. *International Journal of Multiphase Flow*, Vol.10, pp. 61–75.

Peric, M. & Scheuerer, G. (1989). CAST – A Finite Volume Method for Predicting Two-Dimensional Flow and Heat Transfer Phenomena, *GRS – Technische Notiz*, SRR-89-01.

Pfeffer, R.; Rosetti, S. & Licklein, S. (1966). Analysis and Correlation of Heat Transfer Coefficient and Heat Transfer Data for Dilute Gas–Solid Suspensions. *NASA rep. TND-3603*.

van Swaaij, W.P.M. (1985). *Chemical reactors*. Fluidization 2nd Edition, Academic Press, London, UK. (Davidson, J. F., Clift, R. and Harrison, D. Ed.), pp. 595-630.

Sommerfeld, M. (2001). Validation of a stochastic Lagrangian Modelling Approach for Inter-Particle Collisions in Homogeneous Isotropic Turbulence. *International Journal Multiphase Flow*, Vol.27, pp. 1829–1858.

Wang, S.; Liu, H.; Lu, H.; Liu, W.; Jiamin, D. & Li, W. (2005). Flow Behaviour of Clusters in a Riser Simulated by Direct Simulation Monte Carlo Method. *Chemical Engineering Journal*, Vol.106, pp. 197-211.

Zaichik, L. I. & Alipchenkov, V. M. (2005). Statistical Models for Predicting Particle Dispersion and Preferential Concentration in Turbulent Flows. *International Journal of Heat and Fluid Flow*, Vol.26, pp. 416-430.

Thermal Calculation of Power Generators (Standard Method). Moscow, Energija, 1973, 295 pages [in Russian].

Computational Simulations and Applications

Edited by Dr. Jianping Zhu

ISBN 978-953-307-430-6
Hard cover, 560 pages
Publisher InTech
Published online 26, October, 2011
Published in print edition October, 2011

The purpose of this book is to introduce researchers and graduate students to a broad range of applications of computational simulations, with a particular emphasis on those involving computational fluid dynamics (CFD) simulations. The book is divided into three parts: Part I covers some basic research topics and development in numerical algorithms for CFD simulations, including Reynolds stress transport modeling, central difference schemes for convection-diffusion equations, and flow simulations involving simple geometries such as a flat plate or a vertical channel. Part II covers a variety of important applications in which CFD simulations play a crucial role, including combustion process and automobile engine design, fluid heat exchange, airborne contaminant dispersion over buildings and atmospheric flow around a re-entry capsule, gas-solid two phase flow in long pipes, free surface flow around a ship hull, and hydrodynamic analysis of electrochemical cells. Part III covers applications of non-CFD based computational simulations, including atmospheric optical communications, climate system simulations, porous media flow, combustion, solidification, and sound field simulations for optimal acoustic effects.

How to reference

In order to correctly reference this scholarly work, feel free to copy and paste the following:

Alexander Kartushinsky and Andres Siirde (2011). Mathematical Modelling of the Motion of Dust-Laden Gases in the Freeboard of CFB Using the Two-Fluid Approach, Computational Simulations and Applications, Dr. Jianping Zhu (Ed.), ISBN: 978-953-307-430-6, InTech, Available from: http://www.intechopen.com/books/computational-simulations-and-applications/mathematical-modelling-of-the-motion-of-dust-laden-gases-in-the-freeboard-of-cfb-using-the-two-fluid

INTECH
open science | open minds

InTech Europe
University Campus STeP Ri
Slavka Krautzeka 83/A
51000 Rijeka, Croatia
Phone: +385 (51) 770 447
Fax: +385 (51) 686 166
www.intechopen.com

InTech China
Unit 405, Office Block, Hotel Equatorial Shanghai
No.65, Yan An Road (West), Shanghai, 200040, China
中国上海市延安西路65号上海国际贵都大饭店办公楼405单元
Phone: +86-21-62489820
Fax: +86-21-62489821

IntechOpen